ICANS IX

INTERNATIONAL COLLABORATION ON ADVANCED NEUTRON SOURCES

22-26 September, 1986

HIGH RESOLUTION MOLECULAR SPECTROSCOPY USING TFXA AT ISIS

J Penfold

J Tomkinson

Rutherford Appleton Laboratory

Chilton

Didcot

Oxon OX11 0QX

The design and performance of a time focused crystal analyser spectrometer, TFXA, at the ISIS spallation neutron source is presented.

The combination of time and energy focusing provides good (~ 2 to 3%) energy transfer resolution over a wide range of energy transfers (10 to 500 meV).

The influence of multiple scattering on inelastic neutron scattering spectra of molecular vibrations is illustrated with results in hexamethylenetetramine. The capabilities of the spectrometer are illustrated with recent results from the librational mode splitting, of ammonium bromide.

New developments in data analysis using refinable normal coordinate analysis programs are demonstrated with recent data on 1-4 Benzoquinone.

1. Instrument Design

The time-focused crystal analyser, TFXA, is an indirect geometry time-of-flight inelastic scattering spectrometer, using a time-focused pyrolytic graphite analyser to give good count rates, and good energy transfer resolution over a wide range of energy transfers. The design of the spectrometer is illustrated in Figure 1.

The spectrometer is based on a time-focusing geometry in which the sample and detector arrays are in the same plane, and the analysing crystal is set parallel to this plane. In such a geometry, for an ideal crystal, all detected neutrons have the same flight time after scattering. In addition to the time focusing, (2) the Marx principle is used to provide energy focusing. This reduces the positional uncertainty in the analysing energy, and is a feature not previously exploited in crystal analyser spectrometers. It enables the good energy transfer resolution to be maintained down to energy transfers of a few meV.

As the energy of the detected neutrons is small compared with the incident energy, their scattering vector is practically independent of scattering angle. Thus, there can be little variation in the momentum transfer, Q, independent of energy transfer. This is realtively unimportant in molecular vibrational spectroscopy, where the dispersion of the vibrational mode is small or cannot be easily studied. Further, this particular kinematic arrangement renders spectra less sensitive to multiple scattering effects, and as seen later can be exploited to advantage (3).

The simultaneous measurement of the elastic line and a wide range of energy transfers which includes both the internal and external mode vibrations, with good energy transfer resolution offers new possibilities in vibrational spectroscopy.

2. Instrument Performance

During the early running of ISIS, the performance of the TFXA spectrometer was assessed from the vibrational spectra of zirconium hydride (ZrH_2) and potassium hydrogen maleate (KHM). Good resolution and an excellent signal-to-noise performance were observed. Measured intensities were in good agreement with calculation. All aspects of the instrument performed to expectation.

The calibration of the final energy and secondary flight path length values associated with each detector were obtained from the relative positions of the elastic and known inelastic features. The initial calibration using the 140 meV hydrogen vibration of ZrH_2 has been further

refined using the 46.87 meV transition in hexamethylenetetramine (HMT). The elastic line is located at zero energy transfer to within 0.01 meV, and is described by a Gaussian of FWHM of 0.25 meV, in excellent agreement with the calculated elastic resolution. Errors in calibration of peak positions are estimated to be $\leq 0.5\%$.

A number of inelastic features, measured so far, have widths close to the instrumental resolution; for example, the 46.87 meV transition in HMT has a width of 1.12 meV (cf. resolution width of 0.82 meV) and the 144.5 meV vibration in bromoform has a width of 4.6 meV (cf. resolution width of 3.1 meV). For such inelastic features, the line shape in not Gaussian but is described by the characteristic time shape of the ambient water moderator on ISIS.

Early samples have provided a stringent test of data reduction procedures, which present data proportional to cross-section or scattering law in relative or absolute units. Good agreeement with simple harmonic oscillator theory is obtained in these examples, and lends confidence to the data reduction procedures.

Signal-to-noise level is in general excellent. At short times the characteristic break in intensity at the infinite energy channel can be seen.

A detailed analysis of the elastic line shows characteristic wings associated with the thermal diffuse scattering from the pyrolytic analysing crystals.

3. The Influence of Multiple Scattering on Inelastic Neutron Scattering Spectra of Molecular Vibrations (3)

Recent calculations of multiple scattering effects in vibrational spectroscopy suggest that the momentum transfers associated with a TFXA measurement give little weight to multiple phonon scattering effects, i.e. elastic/inelastic, inelastic, and elastic/elastic being the dominant multiple scattering terms. This stems principally from the momentum transfer vector Q being insensitive to scattering angle and determined principally by the energy of the mode being studied, provided it is of

significant energy transfer, for spectrometer with low final energy such as TFXA. To confirm these calculations we have carried out a series of measurements on different percentage scatterers of hexamethylenetetramine, HMT: HMT is a particularly suitable test material as it has a series of sharp well defined modes at relatively low energy transfers.

The measurements confirm the calculations; as is demonstrated in Figure 2 where the ratio $\left(R(\omega)_d\right)$ of scattering from i) 1.9 mm/ 0.9 mm sample thicknesses and ii) 5.4 mm/0.5 mm sample thickness is plotted.

The bold dots correspond to calculated points. The apparent failure of some of the points to correspond with observation is due to the simplicity of the model; in that the external density of states was included only as a delta function, and phonon wings are not included in the calculation.

Figure 3 demonstrates the effect of scattering strength on the observed width of spectral bands. The intense feature at 47 meV is a good candidate for investigation. This band is assigned to ν_{16}, a deformation mode of the carbon-nitrogen skeleton. The width of the ν_{16} band in HMT is the narrowest reported for an NIIS spectrum, 11.5 cm^{-1} [4]. Our spectra from the samples of different scattering strengths were normalised at their peak heights and overplotted. This is shown in Figure 3. It is seen that there is no dramatic increase in band width. Rather a slight broadening at the base. The subtraction of two normalised spectra (strongest minus weakest) is also shown in Figure 3. Here the differences at the base have been strongly emphasised. We may conclude that to first order the widths of spectral bands are independent of scattering strength.

We may conclude for reflection neutron inelastic spectrometers with low final energy, that

i) samples that scatter only 10% of the incident beam are probably inefficient. Neutrons which have been down scattered once can be scattered again, elastically, and are still well described by the one phonon approximation. Total sample scattering strengths of up to 25% are to be recommended for experiments where the inelastic bands occur

at energy transfers greater than 40 meV and relative band intensities are acceptable, i.e. molecular spectroscopy.

ii) Samples that have high scattering strengths continue to show understandable increases in the detected count. These increases arise from multiple inelastic scattering.

Therefore initial experiments of a survey nature on uncharacterised samples are recommended to have scattering strengths, of ca 50%, thereby dramatically reducing the experimental time (by factors of ca 4 to 5).

iii) Degradation of spectral quality will manifest itself by a loss of structure, by weak high energy features becoming less "visible" and by all bands broadening slightly at their base.

4. Splitting of Higher Harmonics of the NH_4^+ Librational Mode in NH_4Br (5)

The rotational motion of ammonium ions in ammonium halides (6) and in the mixed salts of ammonium and alkali halides (7,8) has been extensively studied using the neutron incoherent inelastic scattering (NIIS) technique. These studies show that the librational frequency, ν_6, of the NH_4^+ ion is smaller when the ion resides in an octahedral environment than in a tetrahedral environment. For a given crystal symmetry, ν_6, decreases going from $C\ell^-$ to I^-. The ground librational state of NH_4^+ ions in rock salt alkali halides having symmetry O_h, shows a large (~ 1 meV) tunnel splitting (9) and ν_6 (0-1) gives a broad peak in the scattered neutron spectrum (7,8) indicating that the first excited state also has considerable structure. At appropriately low temperatures, pure ammonium halides have a cubic ordered structure and the NH_4^+ ion resides in a tetrahedral (T_d) environment. In this phase, ν_6 (0-1) gives a sharp peak in neutron experiments. The tunnel splitting of the ground or the higher librational states is expected to be small (10); it is however expected that even in this phase higher librational states may show structure because of the anharmonic effects (11). So far this has not been seen in neutron studies because they were confined to the fundamental ν_6 (0-1) transition. With the availability of high resolution neutron

spectrometers on sources which provide epithermal neutrons, it is now possible to examine the details of the higher excited states. This work reports the first NIIS observation of splitting of the higher overtones of the librational modes of NH_4^+ ions in NH_4Br (Phase IV) (12).

The experiments on polycrystalline ammonium bromide were carried out at a temperature of 6.2 K and the sample scattered 15% of the incident neutrons. The measured scattering law $S(Q,\omega)$ is shown in Figure 4 as a function of energy transfer.

The assignment of various peaks and their comparison with optical data are summarised in Table 1 in particular, the translational optical mode is seen at ~ 20 meV and the fundamental librational mode ν_6 (0-1) at ~ 43 meV. In earlier neutron studies (6) in phase III of NH_4Br, these modes were observed at 20.2 and 41.5 meV respectively. NIIS data on phase IV of NH_4Br have not been previously reported.

Having identified the various peaks, we shall concentrate on ν_6 (0-1) and its harmonics, ν_6 (0-2) and ν_6 (0-3). Expanded plots of the measured spectrum in the region of these modes are shown in Figure 5. We note that both ν_6 (0-2) and ν_6 (0-3) show structure. Thus ν_6 (0-2) consists of two prominent peaks at 81 meV and 86 meV and ν_6 (0-3) consists of two main features at 118 meV and 126 meV. This splitting is not an artifact of acoustic phonon wings. We believe that the splitting of ν_6 (0-2) and ν_6 (0-3) seen in the present experiments is the electrostatic field splitting as predicted by Hüller and Kane (11), and observed for $NH_4C\ell$ in optical experiments (13). We have calcualted the energies of higher librational states for NH_4Br using the formulation developed by Hüller and Kane and the potential suggested by them. The comparison between the calculated and the measured energies is given in Table 1. All the predicted peak positions show excellent agreement with the data. The structure which appears to be present but unresolved in the fundamental region is probably best described in terms of the dispersion of the NH_4^+ librational mode, although the NH_4^+ ion librations in ordered $NH_4C\ell$ showed no dispersion (14).

The integrated relative intensities of the three bands are in very good agreement with the calculations for an oscillator mass of 3.9 neutron

masses, which corresponds to the fact that only hydrogen atoms move during the librational motion and that the NH_4^+ ion has four attached hydrogen atoms.

5. First Observation of the Optically Inactive Modes in Solid 1-4 Benzoquinone (15)

The geometry of 1,4 benzoquinone, shown inset into figure, is though to change markedly on passing from the vapour phase to the solid. Specifically the C=C bond lengths fall from 1.344 Å [16] in the vapour phase to 1.322 Å [17] in the solid. The vibrational spectrum of the molecule should be sensitive to these changes but unfortunately two of the most important vibrations, associated with the C=C deformations, are optically inactive (Au). They have only been observed in the gas phase, and then as weak combinations.

The inelastic incoherent neutron scattering spectrum of 1,4 benzoquinone solid at 20K obtained on TFXA is shown in Figure 6. Also shown is a best fitted valence bond model of the molecular vibrational spectrum. This was achieved using the CLIMAX suite of programs [18]. The same model calculation applied to the gas phase geometry demonstrates that the Au modes are indeed the most sensitive vibrations. However even this sensitivity does not fully explain the large frequency shifts. The most likely explanation is that C-H---O=C contacts, important in crystal formation, are lost on vapourisation.

Acknowledgements

The authors wish to acknowledge the collaboration with P S Goyal on the multiple scattering in HMT, and the splitting of higher harmonics of the NH_4^+ librational mode in NH_4Br.

We wish to thank D K Ross for numerous informative discussions and much useful advice with regard to crystal analyser spectrometers.

We express our gratitude to G J Kearly for making his CLIMAX suite of programs readily available.

References

1. S Ikeda and N Watanabe, Nucl Inst and Meth, 221 (1984) 571.

2. D K Ross, unpublished work.

3. P S Goyal, J Penfold and J Tomkinson, Rutherford Appleton Laboratory report no RAL-86-070.

4. H J Lauter and H Jobic, Chem Phys Lett, 108 (1984) 393.

5. P S Goyal, J Penfold and J Tomkinson, Chem Phys Letters, 127 (1986) 483.

6. G Venkataraman, K Usha Deniz, P K Iyengar, A P Roy and P R Vijayaraghavan, J Phys Chem Solids, 27 (1966) 1103.

7. A B Gardner, T C Waddington and J Tomkinson, J Chem Soc Faraday Trans II, 73 (1977) 1191.

8. P S Goyal and B A Dasannacharya, J Phys, C12 (1979) 219.

9. A Heidemann, J Howard, K J Lushington, J A Morrison, W Press and J Tomkinson, J Phys Soc Japan, 52 (1983) 2401.

10. M Prager, W Press, B Alefeld and A Hüller, J Chem Phys, 67 (1977) 5126.

11. A Hüller and W Kane, J Chem Phys, 61 (1974) 3599.

12. C H Perry and R P Lowndes, J Chem Phys, 51 (1969) 3648.

13. L R Fredrickson and J C Decius, J Chem Phys, 66 (1977) 2297.

14. H C Teh and B N Brockhouse, Phys Rev, 83 (1971) 2733.

15. J Penfold and J Tomkinson, accepted for publication in J Chem Phys.

16. K Hagen and K Hedberg, J Chem Phys, 59 (1973) 158.

17. J Trotter, Acta Cryst, 13 (1960) 86.

18. G J Kearly, J Chem Soc Faraday Trans 2, 82 (1986) 41.

19. N E Schumaker and C G Garland, J Chem Phys, 53 (1970) 392.

Table 1

Summary of the inelastic scattering spectrum of NH_4Br (6K)

This Work (meV)	(10) Theory (meV)	(19) IR Data (meV)	Symmetry Species		
10	--	--		ν_A acoustic branch	translational phonon density
20				ν_o optic branches	of states
43.1	42.4	--	F_2	ν_6 (0→1)	
53	--	49.9		ν_6 (0→1) + ν_A	
62	--	63.2		ν_6 (0→1) + ν_o	
81.0	80.2		A		
84.2	82.95		E	ν_6 (0→2)	
85.7	83.32	83.3	F_2		
118.0	116.4		F_2		
	122.38	122.4	F_2	ν_6 (0→3)	
124.0	122.75		A		
127.0	122.94	125.2	F_2		
145		150.7		ν_6 (0→3) + ν_o	
175	--	173.3	F_2	ν_4 internal NH_4 deformation	

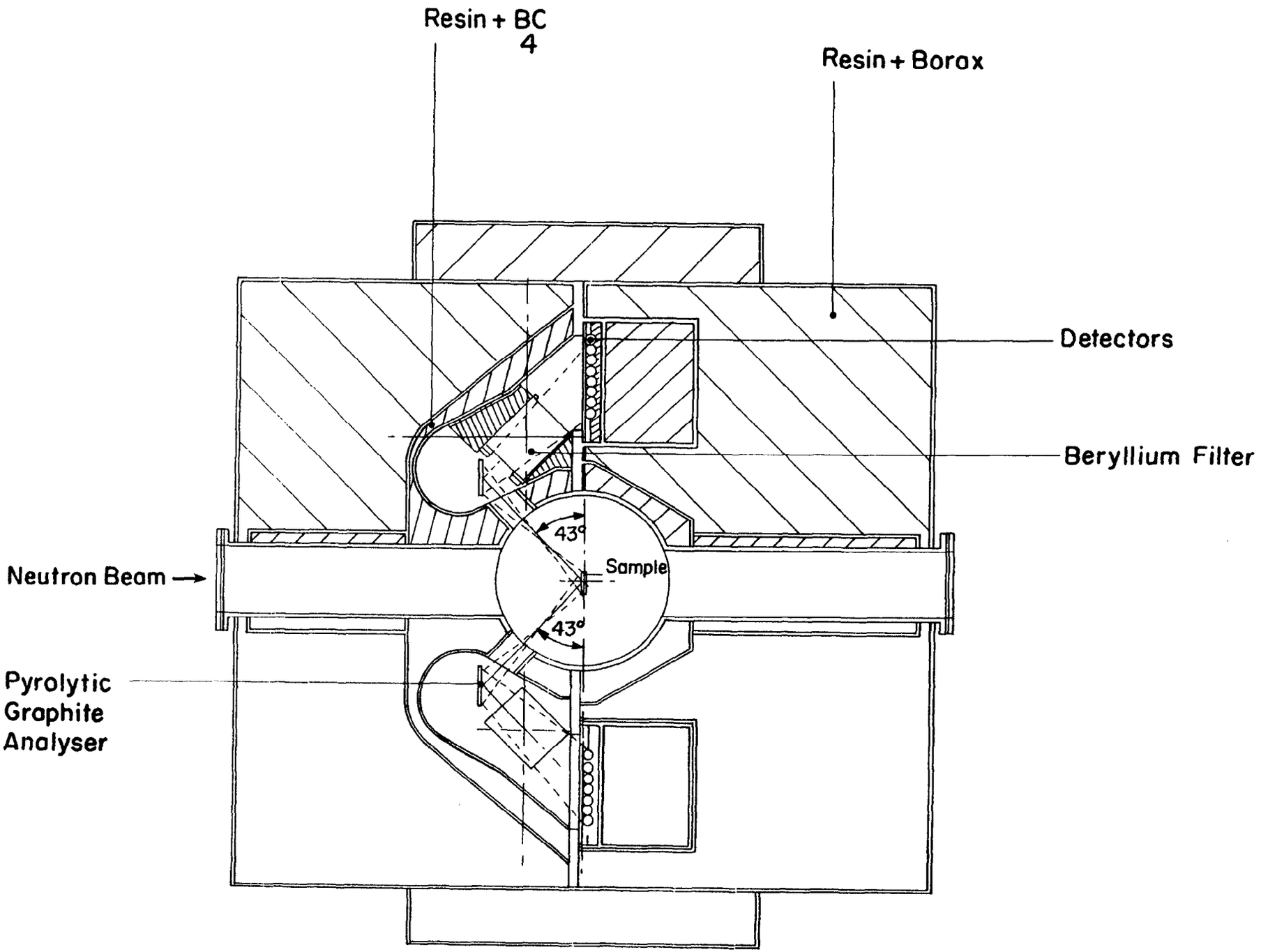

(1) Design of the ISIS time focused crystal analyser TFXA.

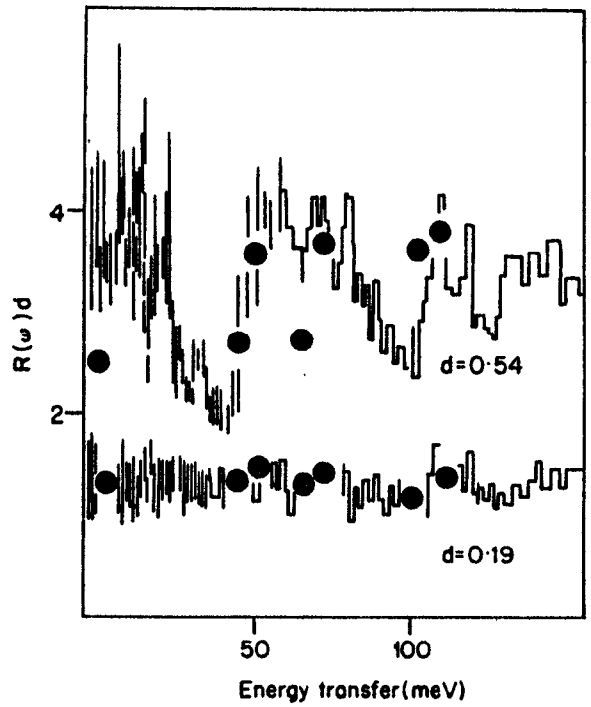

(2) Comparison of the calculated $R(\omega)_d$ values with observation. The calculated points are the bold dots.

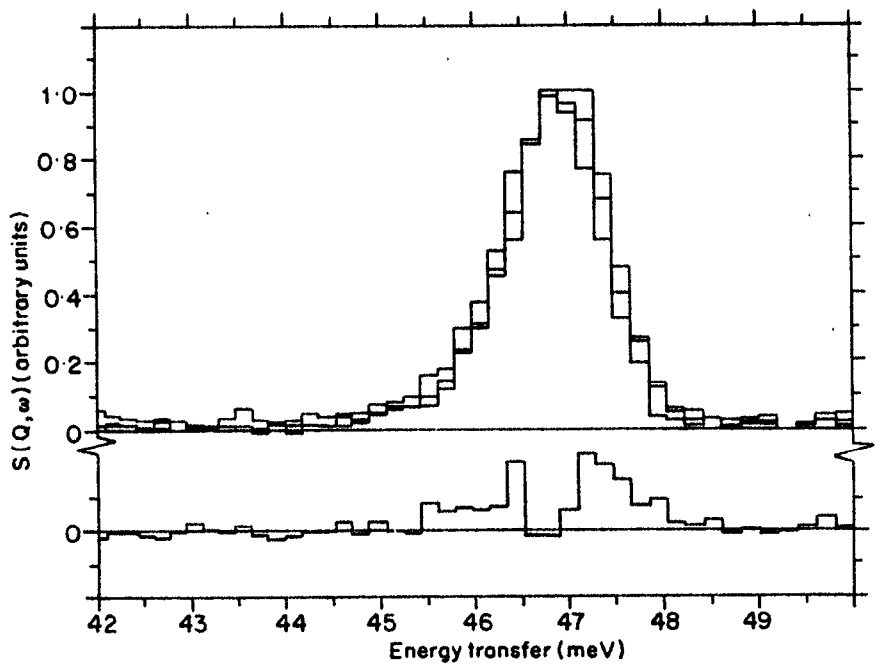

3) Detail of the spectra of HMT around 47 meV neutron energy transfer, showing the normalised observations of ν_{16} mode. Also shown, below, the difference between the normalised results for the thickest and thinnest samples.

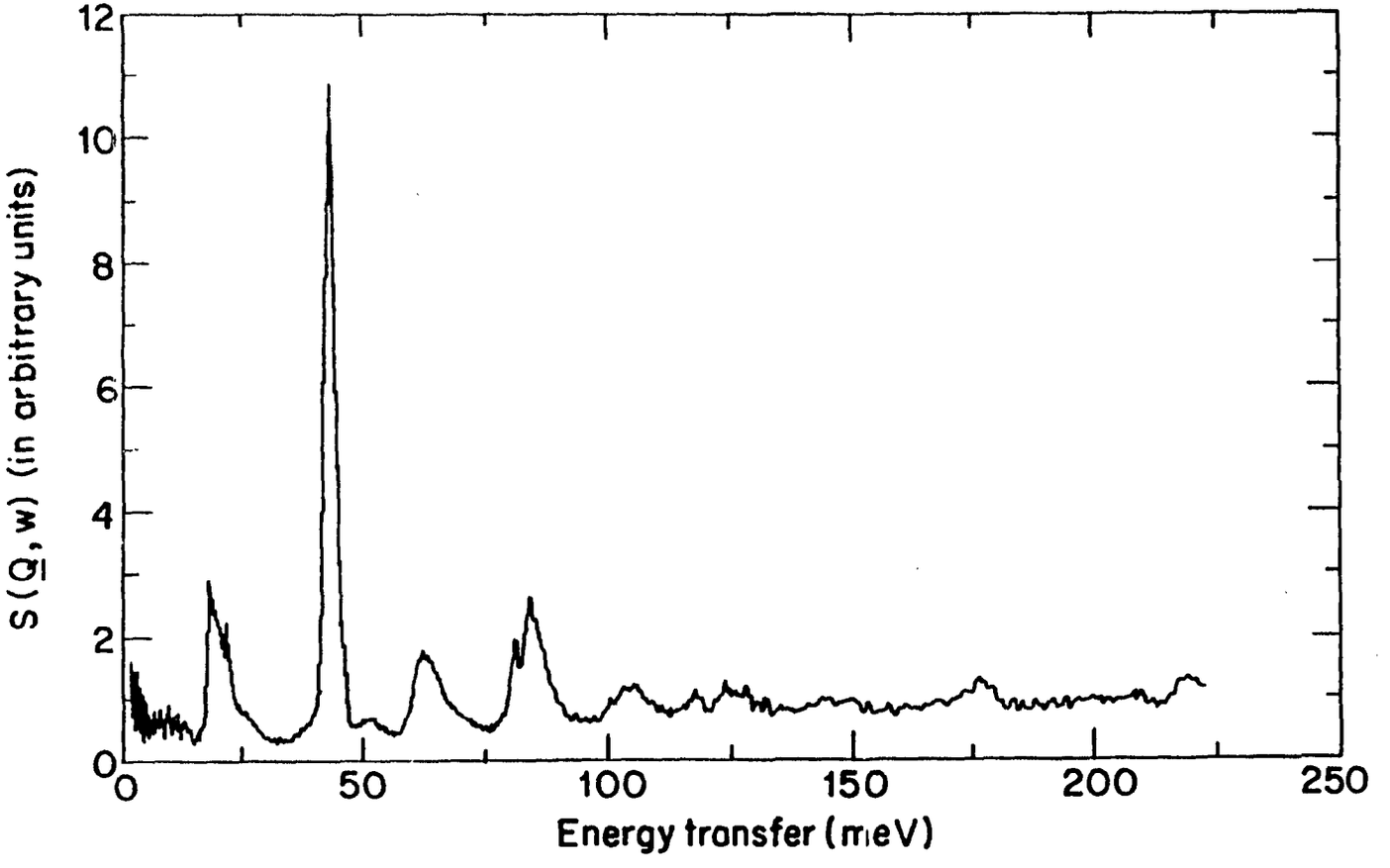

(4) The inelastic incoherent neutron scattering spectrum of NH_4Br at 6K.

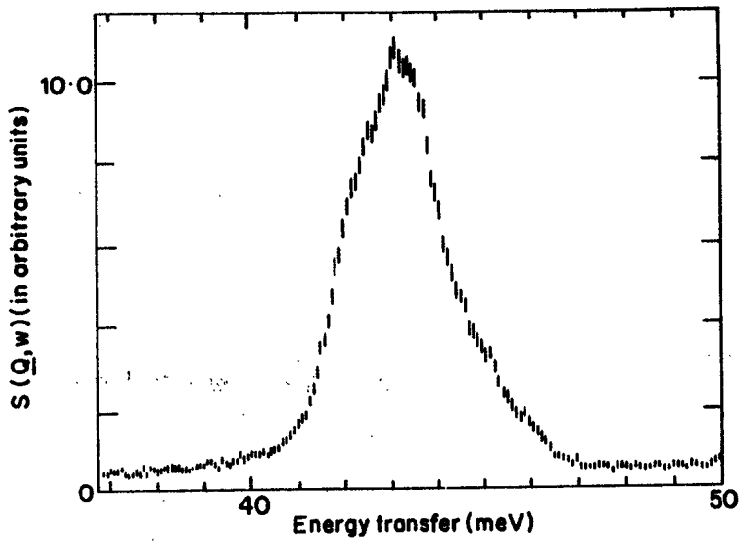

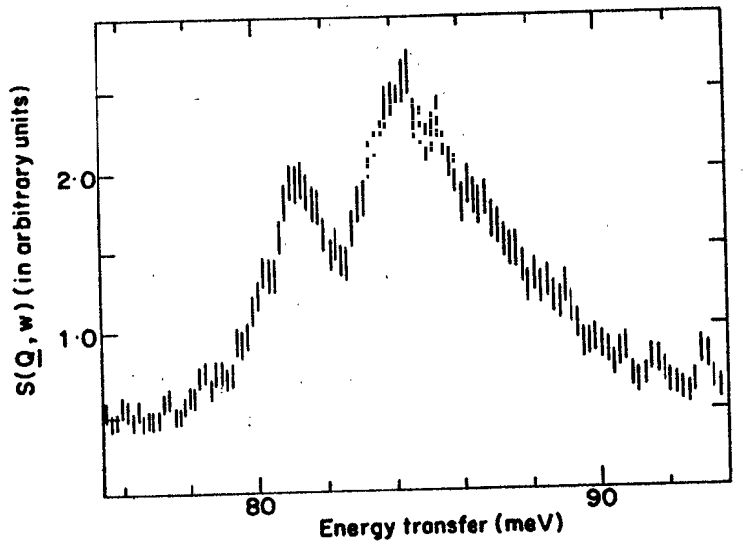

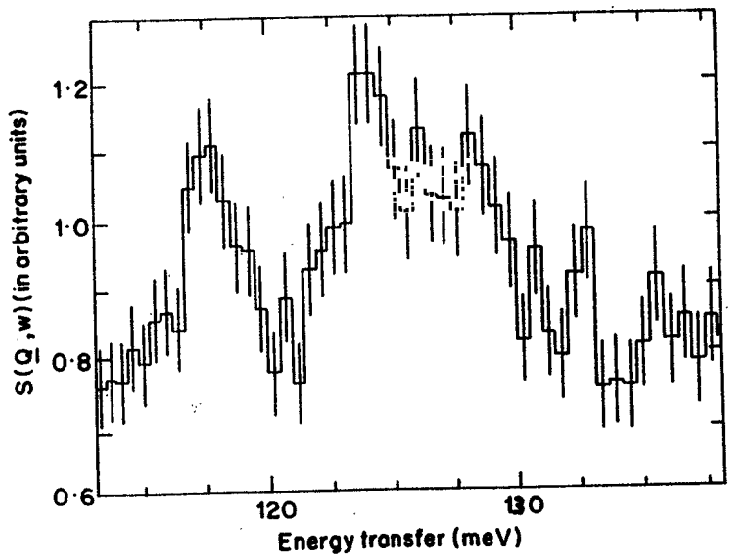

(5) Expanded plots of the NH_4Br spectrum shown in figure covering the 0→1 (a), 0→2 (b) and 0→3 (c) transitions of the librational mode of the ammonium ion.

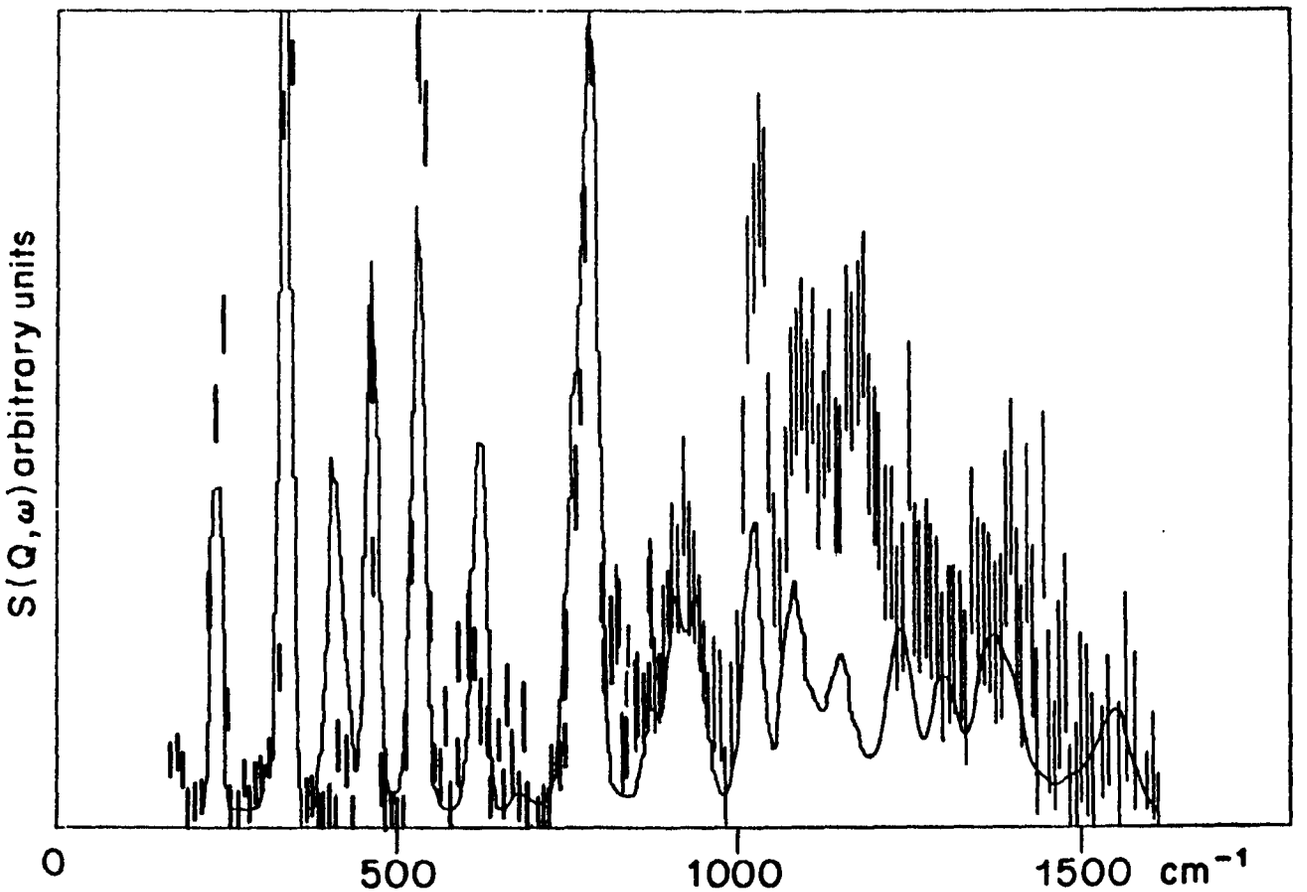

(6) The inelastic incoherent neutron scattering spectrum from 1,4 benzoquinone, at 20K. Only the spectral range from about 200 to 1500 cm^{-1} is shown. The vertical lines represent the data points, with error bars, and the solid line is the best fitted model discussed in the text.